

## Production of monodispersed micron-sized bubbles at high rates in a microfluidic device

Chuanpin Chen,<sup>1,a)</sup> Yonggang Zhu,<sup>1</sup> Patrick W. Leech,<sup>2</sup> and Richard Manasseh<sup>1</sup>

<sup>1</sup>CSIRO Preventative Health National Research Flagship and Fluid Dynamics Group, CSIRO Materials Science and Engineering, P.O. Box 56, Highett, Victoria 3190, Australia

<sup>2</sup>CSIRO Preventative Health National Research Flagship and Wave Physics Group, CSIRO Materials Science and Engineering, Normanby Road, Clayton, Victoria 3168, Australia

(Received 2 June 2009; accepted 11 September 2009; published online 5 October 2009)

A polydimethylsiloxane microchip consisting of a T-junction microchannel network and a thin glass capillary has been developed for the generation of microbubbles. The glass capillary is used to produce an ultrathin gas jet and to controllably block the straight liquid channel, thereby increasing the local liquid velocity near the intersection. Liquid flow rate, liquid viscosity, gas pressure, and inner diameter of the gas jet are varied to investigate the effect on bubble generation. Bubbles with a diameter down to  $4.5\ \mu\text{m}$  can be produced at a high rate of 7.5 kHz using a capillary with an inner diameter of  $2\ \mu\text{m}$ . © 2009 American Institute of Physics. [doi:10.1063/1.3242019]

Microbubbles have many applications in science and engineering. In the field of medical imaging, microbubbles with a diameter of  $1\text{--}10\ \mu\text{m}$  have been used as ultrasound contrast agents. They have also been proposed as drug delivery agents.<sup>1–7</sup> Microbubbles have recently shown the potential to deliver encapsulated drugs across the blood-brain barrier to localized areas of the brain including delivery of large molecules such as the antibody to amyloid- $\beta$ , which is implicated in Alzheimer's disease.<sup>5,6</sup> As an ultrasound contrast agent or ultrasound drug delivery platform, the bubble has to meet the requirements for size and size distribution in ultrasonic imaging.<sup>7</sup> These bubbles must be small enough to pass through the microvasculature without the risk of embolism, while large enough to deliver planned drugs for disease treatment and to generate high sensitivity ultrasonic images in commercial devices.<sup>8–13</sup> The resonant echogenicity of the microbubbles to ultrasound excitation has been reported to vary with bubble diameter to a power of 6.<sup>8,9</sup> Optimal efficiency in ultrasonic imaging has been achieved using microbubbles of a few micrometers in diameter with a narrow size distribution.<sup>13,14</sup>

Microfluidic techniques have provided an alternative means of monodisperse microbubble fabrication. Since the past few years, there has been increasing effort in developing microfluidic devices for dispersing one fluid phase in another immiscible fluid phase, e.g., forming gas bubbles in liquid and water droplets in oil, for new material development and chemical and biological studies.<sup>15–19</sup> Microbubble generation in microchips has been demonstrated by techniques of cross-flow rupturing<sup>7,11,15–17</sup> and coflow hydrodynamic focusing.<sup>8,18</sup> Garstecki *et al.*<sup>19</sup> described a flow-focusing microfluidic device which produced monodisperse bubbles with a diameter of  $10\ \mu\text{m}$ . In flow-focusing devices, the diameter of microbubbles was found to depend on liquid and gas flow rates, liquid viscosity, interfacial tension, and nozzle/channel size.<sup>7,20–26</sup> To produce small bubbles, a reduction in nozzle/channel size is essential for the microfluidic device. However, small size bubbles cannot be generated with a high generation rate.<sup>8</sup> Further, the fabrication of a microchip with

a micron-sized channel is a challenging and costly task since the process requires a high-resolution photolithographic technique.<sup>15</sup> An alternative method is to change the interfacial tension by adding a surfactant to the liquid phase. By lowering the interfacial tension, a smaller gas core stream was formed in the coflow-focusing liquid stream resulting in smaller bubbles.<sup>19</sup> Another method is to use a small inner diameter (ID) capillary gas jet which offers a direct reduction in bubble size for cross-flow rupturing devices. The aim of this letter is to report the development of the capillary gas jet technique for micron-sized bubble formation in microfluidic devices. A prototype microfluidic device combined with a glass capillary, which acted as a gas jet, was fabricated for high throughput generation of microbubbles. The device consisted of a T-junction microchannel network made of polydimethylsiloxane (PDMS) and a thin glass capillary. The flow rate of liquid, liquid viscosity, gas pressure, and the ID of the inserted capillary were varied to study the effect on bubble size, size distribution, and bubble generation rate.

The microfluidic chip was fabricated by a photolithography process and a PDMS molding method.<sup>27</sup> A schematic illustration and a charge coupled device image of the T-junction microchannel network are shown in Fig. 1. The cross-section of the microchannel was  $100 \times 100\ \mu\text{m}^2$ . The straight channel was filled with aqueous phase to act as a cutting jet. The side channel was used for inserting glass capillaries with an ID of  $2\text{--}10\ \mu\text{m}$ . The capillaries were cut to a length of 50 mm and its polymer coating was removed by heating to provide a clear edge with an outer diameter of  $126\ \mu\text{m}$ . The gap between the capillary tip and the straight

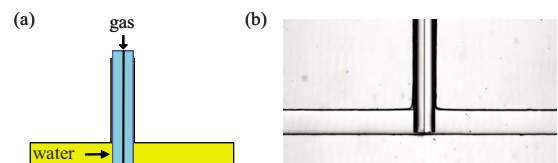


FIG. 1. (Color online) (a) A schematic illustration of a capillary gas jet PDMS microchip for the generation of bubbles using a cross-flow rupturing technique. (b) The image of the PDMS microchip with an inserted capillary. The microchannel cross-section is  $100 \times 100\ \mu\text{m}^2$ , the capillary ID is  $5\ \mu\text{m}$  and OD is  $126\ \mu\text{m}$  without a polymer coating layer.

<sup>a)</sup>Electronic mail: chuanpin.chen@csiro.au.

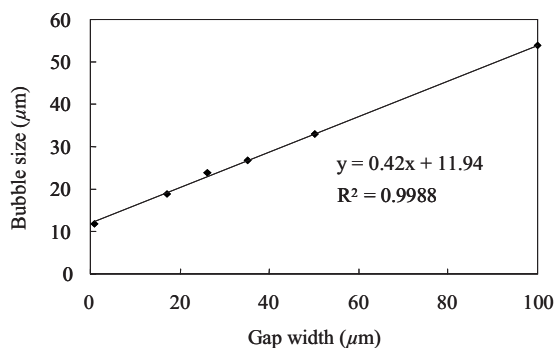


FIG. 2. Bubble size vs the gap between the tip of the glass capillary and the straight channel in the T-junction PDMS microchip. The capillary ID was  $5\ \mu\text{m}$ , the liquid flow rate was  $8\ \text{ml/hr}$  and the gas pressure was  $2\ \text{atm}$ .

channel wall was precisely manipulated under a microscope. After being inserted into the side channel, the capillary was used as a gas jet for bubble formation. The compressed air was pumped through the glass capillary by a syringe. The aqueous phase, [de-ionized water with 5% poly(ethylene glycol) 6000 (PEG6000)], was pumped into the straight channel by a second syringe.

The liquid velocity was varied for bubble formation by controlling the blockage of the straight channel with the insertion of the gas jet capillary. When bubbles grew on the tip of the capillary, the fast flowing liquid played a crucial role to “blow them off” at a small size. However, the increased liquid velocity also induced several problems for bubble generation. Because the hydraulic drag of the liquid was proportional to the flow rate, the high liquid velocity built up a high pressure that caused leakages in the PDMS microchannel. Moreover, the high liquid flow rate had to be combined with a high gas pressure in order to increase the bubble generation rate but this acted to increase bubble size. To address these issues, a technique for enhancing the velocity of the liquid in the gap between the gas jet and the liquid channel without increasing the bulk liquid flow rate was developed. In this microchip, the capillary was inserted into the side channel and was used to partially block the straight channel so that the local liquid velocity at the intersection was increased significantly. Figure 2 shows that the bubble diameter was a linear function of the width of the gap, formed by the  $5\ \mu\text{m}$  ID capillary. For the same liquid flow rate and gas pressure, bubbles formed with a 99% blockage of the straight channel had a diameter of  $11\ \mu\text{m}$ , which was only 20% of the size of bubbles formed in the microchannel without blockage.

The diameter of the bubbles generated in a T-junction configuration was shown to depend on the size of the gas jet in addition to the contribution of gas pressure and liquid flow rate.<sup>28</sup> The minimum size of the microbubbles produced in the T-junction structure was limited by the dimension of the gas jet. In this letter, capillaries with an ID of  $2$ ,  $5$ , and  $10\ \mu\text{m}$  were used as the gas jet nozzles to generate microbubbles with the liquid flow rate of  $8\ \text{ml/hr}$  and gas pressure of  $5\ \text{atm}$ . Bubble images are shown in Fig. 3 for the three capillaries, respectively. The microchip with the  $2\ \mu\text{m}$  ID capillary gas jet generated  $7.8\ \mu\text{m}$  bubbles. The bubble size increased by ninefold when the  $10\ \mu\text{m}$  ID capillary was used.

It was previously reported that a high gas pressure resulted in a high bubble generation rate, while a high liquid flow rate gave a small bubble size.<sup>28</sup> In order to investigate

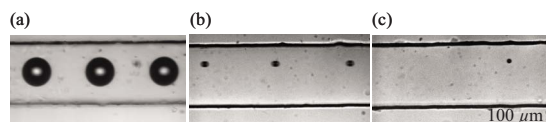


FIG. 3. (Color online) Images of microbubbles generated using glass capillaries with different sizes. The ID of the capillaries was (a)  $10$ , (b)  $5$ , and (c)  $2\ \mu\text{m}$ , respectively. The liquid flow rate was  $8\ \text{ml/hr}$  while the gas pressure was  $5\ \text{atm}$ .

these effects in addition to the effect of liquid viscosity, a series of experiments were performed using a PDMS microchip with a  $5\ \mu\text{m}$  ID capillary gas jet. The liquid viscosity varied from  $0.9$  to  $11\ \text{mPaS}$ , which was achieved by adding PEG6000 to the aqueous phase with different concentrations. The liquid flow rate varied from  $2$  to  $11\ \text{ml/hr}$  while the gas pressure was changed from  $2$  to  $10\ \text{atm}$ . Figure 4(a) shows the bubble size dependence on the liquid flow rate and viscosity at a fixed gas pressure of  $3.3\ \text{atm}$ . The results show that for a given liquid viscosity the bubble size decreased with increasing liquid flow rate. For a set flow rate, the bubble size decreased with increasing viscosity and the change was more pronounced at smaller flow rates.

The effect of gas pressure on the bubble size is shown in Fig. 4(b) for a fixed liquid flow rate of  $8\ \text{ml/hr}$  and the images for the corresponding bubbles are shown in Figs. 4(c)–4(g). At small gas pressures, an increase in gas pressure induced a pronounced increase in bubble size. At large gas pressures ( $>5\ \text{atm}$ ), the bubble size remained almost constant. For example, the bubble size was measured as  $11.8\ \mu\text{m}$  at  $2\ \text{atm}$  with a liquid flow rate of  $8\ \text{ml/hr}$ . If the gas pressure was increased to  $10\ \text{atm}$ , the bubble size was only slightly increased to  $13.4\ \mu\text{m}$ . When the pressure was increased from  $5$  to  $10\ \text{atm}$ , its contribution to bubble size was only 2%. The combination of increased gas pressure and liquid flow rate implies that the generation rate should increase. Indeed, the measurements showed that the bubble generation rate increased by 36-fold when the pressure was increased from  $2$  to  $10\ \text{atm}$ . This finding is significant since the bubble size and generation rate are both crucial parameters in microbubble ultrasound contrast agent fabrication. Production of small microbubbles is necessary to ensure the agents pass through the microvasculature, and a high production rate of the small microbubbles is necessary for practical production.

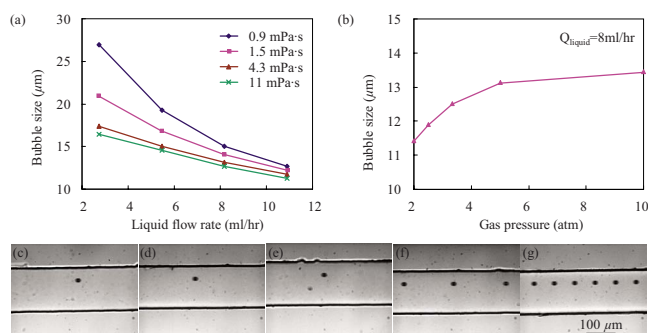


FIG. 4. (Color online) Variation in bubble size with (a) liquid flow rate at different viscosities and (b) gas pressure. (a) The gas pressure was fixed at  $2\ \text{atm}$ . (b) The liquid flow rate was  $8\ \text{ml/h}$ . The images of bubbles generated from the  $5\ \mu\text{m}$  ID capillary for the five gas pressures are shown in (c)  $2$ , (d)  $2.5$ , (e)  $3.33$ , (f)  $5$ , and (g)  $10\ \text{atm}$ , respectively. All the images were taken from the midpoint of the straight channel in the microchip.

In the gas jet microchip with a 2  $\mu\text{m}$  ID capillary, the effect of gas pressure on bubble size was small. There was little change in the bubble diameter when the gas pressure was changed from 3 to 10 atm. The bubbles with a diameter of 4.5  $\mu\text{m}$  were produced when a high force syringe pump was used to increase the liquid flow rate up to 16 ml/hr. A generation rate of 2.3 kHz was achieved when the gas pressure was set at 3 atm. Such a rate was increased to 7.5 kHz when the pressure was increased to 10 atm.

In summary, the capillary gas jet microchip has been developed for microbubble generation by a cross-flow rupturing method. A controlled partial blockage of the liquid flow resulted in a significant increase in the local velocity of the liquid. Monodisperse microbubbles could be generated at a high frequency using a combination of high liquid flow rate and high gas pressure. The bubble diameter could be down to 4.5  $\mu\text{m}$  when a 2  $\mu\text{m}$  ID capillary was used. Combined with the technique of lipid coating, these microbubbles can potentially be produced in a more stable state for the applications of ultrasound imaging and drug encapsulation.

- <sup>1</sup>R. Manasseh and A. Ooi, *Bubble Science, Engineering & Technology* **1**, 58 (2009).
- <sup>2</sup>E. Stride and M. Edirisinghe, *Soft Matter* **4**, 2350 (2008).
- <sup>3</sup>C.-D. Ohl and B. Wolfrum, *Biochim. Biophys. Acta* **1624**, 131 (2003).
- <sup>4</sup>K. Ferrara, R. Pollard, and M. Borden, *Annu. Rev. Biomed. Eng.* **9**, 415 (2007).
- <sup>5</sup>J. J. Choi, M. Pernot, T. R. Brown, S. A. Small, and E. E. Konofagou, *Phys. Med. Biol.* **52**, 5509 (2007).
- <sup>6</sup>S. B. Raymond, L. H. Treat, J. D. Dewey, N. J. McDannold, K. Hynynen, and B. J. Bacskaï, *PLoS ONE* **3**, 1 (2008).
- <sup>7</sup>J. H. Xu, G. S. Luo, S. W. Li, and G. G. Chen, *Lab Chip* **6**, 131 (2006).
- <sup>8</sup>K. Hettiarachchi, E. Talu, M. L. Longo, P. A. Dayton, and A. P. Lee, *Lab Chip* **7**, 463 (2007).
- <sup>9</sup>M. B. Butler, D. H. Thomas, S. D. Pye, C. M. Moran, W. N. McDicken, and V. Sboros, *Appl. Phys. Lett.* **93**, 223906 (2008).
- <sup>10</sup>Y. Liu, H. Miyoshi, and M. Nakamura, *J. Controlled Release* **114**, 89 (2006).
- <sup>11</sup>J. H. Xu, S. W. Li, Y. J. Wang, and G. S. Luo, *Appl. Phys. Lett.* **88**, 133506 (2006).
- <sup>12</sup>A. M. Gañán-Calvo and J. M. Gordillo, *Phys. Rev. Lett.* **87**, 274501 (2001).
- <sup>13</sup>K. Pancholi, U. Farook, R. Moaleji, E. Stride, and M. Edirisinghe, *Eur. Biophys. J.* **37**, 515 (2008).
- <sup>14</sup>A. Klibanov, *Contrast Agents II*, Ultrasound Contrast Agents: Development of the Field and Current Status (Springer, Berlin, 2002), p. 76.
- <sup>15</sup>Y. Zhu and B. E. Power, *Adv. Biochem. Eng./Biotech.* **110**, 81 (2008).
- <sup>16</sup>H. Shintaku, S. Imamura, and S. Kawano, *Exp. Therm. Fluid Sci.* **32**, 1132 (2008).
- <sup>17</sup>W. Zhang and R. B. H. Tan, *Chem. Eng. Sci.* **58**, 287 (2003).
- <sup>18</sup>W. Zhang and R. B. H. Tan, *Chem. Eng. Sci.* **55**, 6243 (2000).
- <sup>19</sup>P. Garstecki, I. Gitlin, W. Diluzio, G. M. Whitesides, E. Kumacheva, and H. A. Stone, *Appl. Phys. Lett.* **85**, 2649 (2004).
- <sup>20</sup>A. Kulkarni and J. B. Joshi, *Ind. Eng. Chem. Res.* **44**, 5873 (2005).
- <sup>21</sup>M. Weber and R. Shandas, *Microfluid. Nanofluid.* **3**, 195 (2007).
- <sup>22</sup>Z. Xiao and R. B. H. Tan, *Chem. Eng. Sci.* **60**, 179 (2005).
- <sup>23</sup>L. Klibanov, *Bioconjugate Chem.* **16**, 9 (2005).
- <sup>24</sup>E. Talu, M. M. Lozano, R. L. Powell, P. A. Dayton, and M. L. Longo, *Langmuir* **22**, 9487 (2006).
- <sup>25</sup>G. I. Taylor, *Proc. R. Soc. London, Ser. A* **146**, 501 (1934).
- <sup>26</sup>B. Dollet, W. van Hoeve, J.-P. Raven, P. Marmottant, and M. Versluis, *Phys. Rev. Lett.* **100**, 034504 (2008).
- <sup>27</sup>C. Chen and J. H. Hahn, *Anal. Chem.* **79**, 7182 (2007).
- <sup>28</sup>P. Garstecki, M. J. Fuerstman, H. A. Stone, and G. M. Whitesides, *Lab Chip* **6**, 437 (2006).